Comparative Study of IDR and BiCG variant methods in Numerical Analysis Based on Method of Moments

Hidetoshi Chiba[1], Toru Fukasawa[1], and Hiroaki Miyashita[1]
[1] Antennas Technology Department, Mitsubishi Electric Corporation, 5-1-1 Ofuna, Kamakura, Kanagawa 247-8501, Japan

***Abstract* - In this study, we investigate the performance of the variants of the induced dimension reduction (IDR) in large-scale electromagnetic scattering problems. Comparative numerical experiments, using IDR(s), GIDR(s, L), and ML(s)BiCGSTAB reveal that GIDR(s, L) shows the fastest convergence property among the three IDR variants. In a numerical experiment with a practical radiation problem, GIDR(s, L) with an s value of around 15 shows the best performance with respect to the balance between the convergence property and the tolerance to the spurious convergence.**

***Index Terms* — IDR variant methods, BiCG variant methods, Method of moments, Fast multipole method.**

I. INTRODUCTION

In recent years, one of the Krylov subspace methods, i.e., the induced dimension reduction (IDR) method, has attracted considerable attention in the field of computational physics. In 2007, Sonneveld and van Gijzen reconsidered the IDR method and generalized it to the IDR(*s*) method [1]. Besides, by using higher-order stabilization polynomials, IDR(*s*)stab(*L*) and GIDR(*s*, *L*) were derived by Tanio[2] in 2009. Also, as Tanio stated, ML(*s*)BiCGSTAB can be considered as one of the IDR variant methods. The main objective of this study is to investigate and clarify the convergence performance of the IDR variant methods, i.e., IDR(*s*), GIDR(*s*, *L*), and ML(*s*)BiCGSTAB implemented along with the method of moments (MoM).

II. IDR VARIANT METHODS

The unique feature of the IDR(*s*) method is that the residual vector converges to a zero vector because the dimensions of the spaces to which the residual vector belongs decrease monotonically, in accordance with the IDR theorem. Mathematically, it requires at most $N + N/s$ matrix-vector multiplications (MATVEC) to obtain the exact solution, while Bi-CG based methods need $2N$ MATVEC.

Meanwhile, IDR-variants possess an inherent problem, the so-called "spurious convergence". It is a phenomenon where the true relative residual norm (TRRN) at convergence becomes much larger than the value of the predefined tolerance. Recently, the performance of these IDR variants has been investigated in several numerical tests of the applied physics; however, thus far, it has hardly been studied or used for electromagnetic wave problems. Against this background, in the following sections, we investigate the convergence performance and tolerance to the spurious convergence of the IDR variant methods, i.e., IDR(*s*), GIDR(*s*, *L*), and ML(*s*)BiCGSTAB, through a numerical experiment with a practical electromagnetic radiation problem.

III. NUMERICAL EXPERIMENTS

We consider a practical problem of a horn antenna radiating in the presence of a radome equipped with a frequency selective surface (FSS). Fig. 1 displays the geometry of the antenna and radome. The antenna is assumed to be a standard gain horn. An FSS-embedded radome, having the shape of a partial sphere with a radius at the radome base of 12λ, is placed in front of the antenna aperture. The radome wall profile and the unit cell of the FSS layer are depicted in Figs. 2(a) and 2(b). The dielectric layers are assumed to have the so-called "A-sandwich" structure, with two skin layers (ε_r = 4.277 and $\tan\delta$ = 1.695E-2) separated by a core layer (ε_r = 1.167 and $\tan\delta$ = 0.814E-2). As shown in Fig. 2(a), an FSS layer, which consists of a square-grid arrangement of ring-shaped slots on a conducting surface, is embedded in each of the two skin layers. Fig. 3 exhibits a photograph of the fabricated FSS-embedded radome. This geometry is discretized into 444,064 triangles, and the resultant linear system has 1,013,744 degrees of freedom. For the implementation of the MoM, we employ a combined tangential formulation (CTF) [3], and the multilevel fast multipole algorithm (MLFMA) was incorporated. We use the RWG basis functions [4] for surface current expansion. We conduct comparative experiments with IDR(*s*), GIDR(*s*, *L*), ML(*s*)BiCGSTAB. We use two stopping criteria for iterative solvers: a tolerance of 1.0E-4 and a maximum iteration number of 5,000. In addition, diagonal scaling is applied to all the solvers. All the runs are performed in double precision on an Itanium 2 processor on an SGI Altix 450 server.

Table I summarizes the numerical results of the number of MATVEC and TRRN, and Fig. 4 depicts convergence histories for the three IDR-variants. Also, for comparison purpose, Table I includes the results for the restarted

generalized minimal residual (GMRES(*m*)) algorithm [5] . From the results, the following facts have been clarified:

- As for the convergence rate, GIDR(*s*, *L*) with *s* set to around 15 performs best among all the methods. ML(s)BiCGSTAB converges slightly slow as compared to other methods.
- From the results of TRRN, GIDR(*s*, *L*) with large *s* suffers from the spurious convergence, while IDR(*s*) and ML(*s*)BiCGSTAB are stable regardless of the setting of *s*.

In term of the memory usage, IDR-variant methods consume less memory than does GMRES(*m*).

IV. Conclusion

In this paper, we investigated the performance of the IDR variant methods in an electromagnetic radiation problem involving a practical geometry. Numerical experiments revealed that GIDR(*s*, *L*) with appropriately selected *s* and *L*, showed a predominant convergence property as compared to other methods and GIDR(*s*, *L*) with an *s* value of around 15 gives the best performance with respect to the balance between the convergence property and the tolerance to spurious convergence.

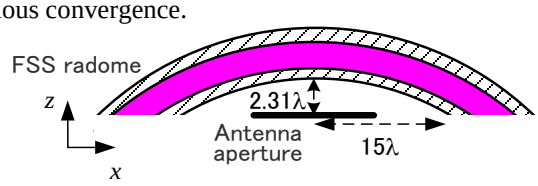

Fig. 1. Geometry of the aperture of the standard gain horn antenna covered with the FSS- embedded radome.

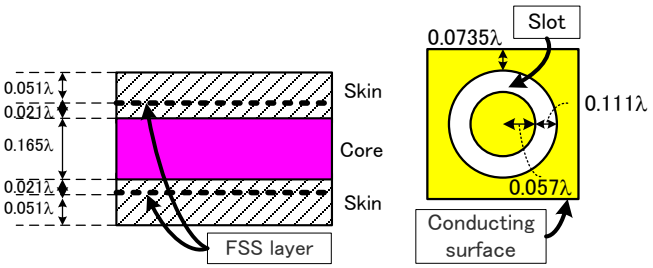

(a) Radome wall profile (b) Unit cell of FSS the layer

Fig. 2. Radome wall profile and a unit cell of the FSS layer.

Fig. 3. A photograph of the fabricated FSS-embedded radome that was used for the measurement.

References

[1] P. Sonneveld and M. B. van Gijzen, "IDR(s): A family of simple and fast algorithms for solving large nonsynmetric linear systems," SIAM J. Sci. Comp., vol. 31, pp. 1035–1062, 2007.

[2] M. Tanio and M. Sugihara, "GBi-CGSTAB(s, L): IDR(s) with higher-order stabilization polynomials," Mathematical Engineering Technical Reports, The University of Tokyo, METR2009-16, 2009.

[3] Ö. Ergül and L. Gürel, "Comparison of integral-equation formulations for the fast and accurate solution of scattering problems involving dielectric objects with the multilevel fast multipole algorithm," IEEE Trans. Antennas Propagat., vol. 57, no. 1, pp. 176–187, Jan. 2009.

[4] S. M. Rao, D. R. Wilton, and A. W. Glisson, "Electromagnetic scattering by surfaces of arbitrary shape," IEEE Trans. Antennas Propagat., vol. AP-30, no. 3, pp. 409–418, May 1982.

[5] Y. Saad and M. H. Schultz, "GMRES: A generalized minimal residual algorithm for solving nonsymmetric linear systems," SIAM J. Sci. Stat. Comput., vol. 7, no. 3, pp. 856–869, July 1986.

TABLE I
Numerical Results of the Numerical Experiments.

手法	L	s	MATVEC	TRRN	Memory [GB]
IDR(s)	-	10	2896	9.650e-05	56.3
		20	2610	9.536e-05	56.7
		30	3941	7.616e-05	57.1
GIDR(s,L)	2	10	2716	8.580e-05	56.5
		20	2540	8.248e-05	57.1
		30	3440	4.067e-04	57.6
	4	10	2324	9.724e-05	57.3
		20	2372	8.750e-05	58.1
		30	3562	2.402e-03	59.0
ML(s)BICGSTAB	-	10	3884	8.737e-05	56.6
		50	4127	8.703e-05	58.2
		100	4441	9.535e-05	60.2
GMRES(s)	-	10	N.C.	-	56.4
		50	4597	9.930e-05	58.4
		100	2163	9.991e-05	60.8

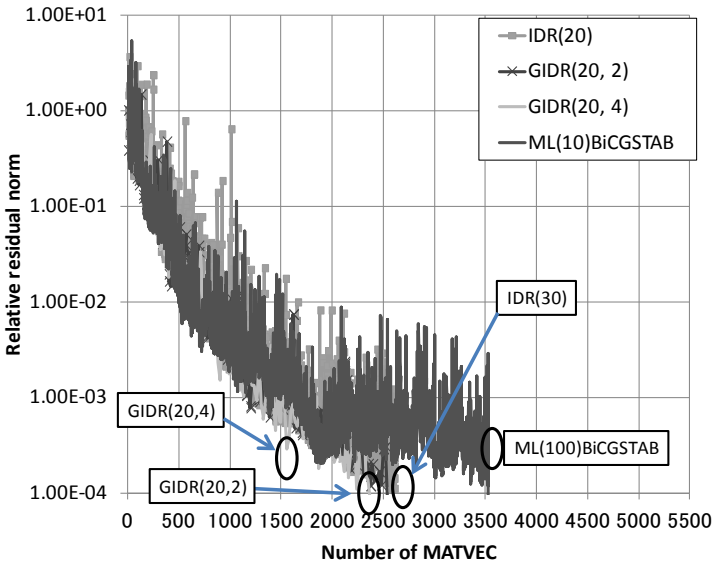

Fig. 4. Convergence histories for IDR(s), GIDR(s, L) and ML(s)BiCGSTAB.